The limitation of this study was the small number of subjects enrolled and the relatively short follow-up period (1 year). Increasing the number of subjects is required to make a more robust conclusion about the association of the *CD36* gene with the outcome of PDT. Since evaluating the association of *CD36* variants with the durability of the PDT effect is important, further investigations with an extended follow-up period are needed.

Since PDT is known to induce several gene expression changes in the retina-choroidal complex [42], the detailed mechanisms by which multiple genes interact with each other to close the CNV are poorly understood. However, the present study suggested some clinical possibilities for genetic association analysis, which can be further investigated to determine the specific molecules involved in the mechanism(s) responsible for the actions of PDT, and may give genetic information that can be applied for personalized therapies in individual patients with PCV.

ACKNOWLEDGMENTS

This study was supported by a Grant-in Aid (C) 23,592,567 from the Ministry of Education, Science and Culture, Tokyo, Japan (S.H.), and by a grant from the Takeda Science Foundation, Osaka, Japan (S.H.). The funding organization had no role in the design or conduct of this research. The authors have no proprietary or commercial interest in any of the materials discussed in this article.

REFERENCES

1. Maruko I, Iida T, Saito M, Nagayama D, Saito K. Clinical characteristics of exudative age-related macular degeneration in Japanese patients. Am J Ophthalmol 2007; 144:15-22. [PMID: 17509509].
2. Liu Y, Wen F, Huang S, Luo G, Yan H, Sun Z, Wu D. Subtype lesions of neovascular age-related macular degeneration in Chinese patients. Graefes Arch Clin Exp Ophthalmol 2007; 245:1441-5. [PMID: 17406882].
3. Yannuzzi LA, Sorenson J, Spaide RF, Lipson B. Idiopathic polypoidal choroidal vasculopathy (IPCV). Retina 1990; 10:1-8. [PMID: 1693009].
4. Ciardella AP, Donsoff IM, Huang SJ, Costa DL, Yannuzzi LA. Polypoidal choroidal vasculopathy. Surv Ophthalmol 2004; 49:25-37. [PMID: 14711438].
5. Yannuzzi LA, Wong DW, Sforzolini BS, Goldbaum M, Tang KC, Spaide RF, Freund KB, Slakter JS, Guyer DR, Sorenson JA, Fisher Y, Maberley D, Orlock DA. Polypoidal choroidal vasculopathy and neovascularized age-related macular degeneration. Arch Ophthalmol 1999; 117:1503-10. [PMID: 10565519].
6. Bessho H, Honda S, Imai H, Negi A. Natural course and funduscopic findings of polypoidal choroidal vasculopathy in a Japanese population over 1 year of follow-up. Retina 2011; 31:1598-602. [PMID: 21478804].
7. Honda S, Kurimoto Y, Kagotani Y, Yamamoto H, Takagi H, Uenishi M. Hyogo Macular Disease Study Group. Photodynamic therapy for typical age-related macular degeneration and polypoidal choroidal vasculopathy: a 30-month multicenter study in Hyogo, Japan. Jpn J Ophthalmol 2009; 53:593-7. [PMID: 20020237].
8. Honda S, Imai H, Yamashiro K, Kurimoto Y, Kanamori-Matsui N, Kagotani Y, Tamura Y, Yamamoto H, Ohoto S, Takagi H, Uenishi M, Negi A. Comparative assessment of photodynamic therapy for typical age-related macular degeneration and polypoidal choroidal vasculopathy: a multicenter study in Hyogo prefecture, Japan. Ophthalmologica 2009; 223:333-8. [PMID: 19478533].
9. Byeon SH, Lew YJ, Lee SC, Kwon OW. Clinical features and follow-up results of pulsating polypoidal choroidal vasculopathy treated with photodynamic therapy. Acta Ophthalmol 2010; 88:660-8. [PMID: 19563374].
10. Tsuchihashi T, Mori K, Horie-Inoue K, Gehlbach PL, Kabasawa S, Takita H, Ueyama K, Okazaki Y, Inoue S, Awata T, Katayama S, Yoneya S. Complement factor H and high-temperature requirement A-1 genotypes and treatment response of age-related macular degeneration. Ophthalmology 2011; 118:93-100. [PMID: 20678803].
11. Sakurada Y, Kubota T, Imasawa M, Mabuchi F, Tanabe N, Iijima H. Association of LOC387715 A69S genotype with visual prognosis after photodynamic therapy for polypoidal choroidal vasculopathy. Retina 2010; 30:1616-21. [PMID: 20671585].
12. Bessho H, Honda S, Kondo N, Negi A. The association of *ARMS2* polymorphisms with phenotype in typical neovascular age-related macular degeneration and polypoidal choroidal vasculopathy. Mol Vis 2011; 17:977-82. [PMID: 21541271].
13. Silverstein RL, Febbraio M. CD36, a scavenger receptor involved in immunity, metabolism, angiogenesis, and behavior. Sci Signal 2009; 2:re3-[PMID: 19471024].
14. Febbraio M, Hajjar DP, Silverstein RL. CD36: a class B scavenger receptor involved in angiogenesis, atherosclerosis, inflammation, and lipid metabolism. J Clin Invest 2001; 108:785-91. [PMID: 11560944].
15. Kuniyasu A, Ohgami N, Hayashi S, Miyazaki A, Horiuchi S, Nakayama H. CD36-mediated endocytic uptake of advanced glycation end products (AGE) in mouse 3T3–L1 and human subcutaneous adipocytes. FEBS Lett 2003; 537:85-90. [PMID: 12606036].
16. Kociok N, Joussen AM. Varied expression of functionally important genes of RPE and choroid in the macula and in the periphery of normal human eyes. Graefes Arch Clin Exp Ophthalmol 2007; 245:101-13. [PMID: 16598467].

17. van den Bergh H. Photodynamic therapy of age-related macular degeneration: History and principles. Semin Ophthalmol 2001; 16:181-200. [PMID: 15513440].

18. Kondo N, Honda S, Kuno S, Negi A. Positive Association of Common Variants in *CD36* with Neovascular Age-Related Macular Degeneration. Aging 2009; 1:266-74. [PMID: 20157514].

19. Bessho H, Honda S, Kondo N, Kusuhara S, Tsukahara Y, Negi A. The association of *CD36* variants with polypoidal choroidal vasculopathy compared to typical neovascular age-related macular degeneration. Mol Vis 2012; 18:121-7. [PMID: 22275803].

20. Picard E, Houssier M, Bujold K, Sapieha P, Lubell W, Dorfman A, Racine J, Hardy P, Febbraio M, Lachapelle P, Ong H, Sennlaub F, Chemtob S. CD36 plays an important role in the clearance of oxLDL and associated age-dependent sub-retinal deposits. Aging (Albany NY) 2010; 2:981-9. [PMID: 21098885].

21. Scott LJ, Goa KL. Verteporfin. Drugs Aging 2000; 16:139-46. , discussion 147–8.. [PMID: 10755329].

22. . Japanese Study Group of Polypoidal Choroidal Vasculopathy. Criteria for diagnosis of polypoidal choroidal vasculopathy Nippon Ganka Gakkai Zasshi 2005; 109:417-27. in Japanese[PMID: 16050460].

23. . Treatment of Age-Related Macular Degeneration with Photodynamic Therapy (TAP) Study Group. Photodynamic therapy of subfoveal choroidal neovascularization in age-related macular degeneration with verteporfin. One-year results of 2 randomized clinical trials: TAP report 1. Arch Ophthalmol 1999; 117:1329-45. [PMID: 10532441].

24. . The International HapMap Consortium. The International HapMap Project. Nature 2003; 426:789-96. [PMID: 14685227].

25. de Bakker PI, Yelensky R, Pe'er I, Gabriel SB, Daly MJ, Altshuler D. Efficiency and power in genetic association studies. Nat Genet 2005; 37:1217-23. [PMID: 16244653].

26. Nakata I, Yamashiro K, Yamada R, Gotoh N, Nakanishi H, Hayashi H, Tsujikawa A, Otani A, Ooto S, Tamura H, Saito M, Saito K, Iida T, Oishi A, Kurimoto Y, Matsuda F, Yoshimura N. Genetic variants in pigment epithelium-derived factor influence response of polypoidal choroidal vasculopathy to photodynamic therapy. Ophthalmology 2011; 118:1408-15. [PMID: 21439646].

27. Wu K, Wen F, Zuo C, Li M, Zhang X, Chen H, Zeng R. Lack of association with PEDF Met72Thr variant in neovascular age-related macular degeneration and polypoidal choroidal vasculopathy in a Han Chinese population. Curr Eye Res 2012; 37:68-72. [PMID: 22029535].

28. Nakata I, Yamashiro K, Yamada R, Gotoh N, Nakanishi H, Hayashi H, Tsujikawa A, Otani A, Saito M, Iida T, Oishi A, Matsuo K, Tajima K, Matsuda F, Yoshimura N. Association between the SERPING1 gene and age-related macular degeneration and polypoidal choroidal vasculopathy in Japanese. PLoS ONE 2011; 6:e19108-[PMID: 21526158].

29. Li M, Wen F, Zuo C, Zhang X, Chen H, Huang S, Luo G. SERPING1 polymorphisms in polypoidal choroidal vasculopathy. Mol Vis 2010; 16:231-9. [PMID: 20161815].

30. Bessho H, Kondo N, Honda S, Kuno S, Negi A. Coding variant Met72Thr in the PEDF gene and risk of neovascular age-related macular degeneration and polypoidal choroidal vasculopathy. Mol Vis 2009; 15:1107-14. [PMID: 19503741].

31. Gotoh N, Yamada R, Nakanishi H, Saito M, Iida T, Matsuda F, Yoshimura N. Correlation between CFH Y402H and HTRA1 rs11200638 genotype to typical exudative age-related macular degeneration and polypoidal choroidal vasculopathy phenotype in the Japanese population. Clin Experiment Ophthalmol 2008; 36:437-42. [PMID: 18939352].

32. Sakurada Y, Kubota T, Imasawa M, Tsumura T, Mabuchi F, Tanabe N, Iijima H. Angiographic lesion size associated with LOC387715 A69S genotype in subfoveal polypoidal choroidal vasculopathy. Retina 2009; 29:1522-6. [PMID: 19898184].

33. Khandhadia S, Lotery A. Oxidation and age-related macular degeneration: insights from molecular biology. Expert Rev Mol Med 2010; 12:e34-[PMID: 20959033].

34. Plafker SM. Oxidative stress and the ubiquitin proteolytic system in age-related macular degeneration. Adv Exp Med Biol 2010; 664:447-56. [PMID: 20238046].

35. Houssier M, Raoul W, Lavalette S, Keller N, Guillonneau X, Baragatti B, Jonet L, Jeanny JC, Behar-Cohen F, Coceani F, Scherman D, Lachapelle P, Ong H, Chemtob S, Sennlaub F. CD36 deficiency leads to choroidal involution via COX2 down-regulation in rodents. PLoS Med 2008; 5:e39-[PMID: 18288886].

36. Yamada Y, Tian J, Yang Y, Cutler RG, Wu T, Telljohann RS, Mattson MP, Handa JT. Oxidized low density lipoproteins induce a pathologic response by retinal pigmented epithelial cells. J Neurochem 2008; 105:1187-97. [PMID: 18182060].

37. Kamei M, Yoneda K, Kume N, Suzuki M, Itabe H, Matsuda K, Shimaoka T, Minami M, Yonehara S, Kita T, Kinoshita S. Scavenger receptors for oxidized lipoprotein in age-related macular degeneration. Invest Ophthalmol Vis Sci 2007; 48:1801-7. [PMID: 17389514].

38. Scott LJ, Goa KL. Verteporfin. Drugs Aging 2000; 16:139-46. , discussion 147–8.. [PMID: 10755329].

39. Yuan HY, Chiou JJ, Tseng WH, Liu CH, Liu CK, Lin YJ, Wang HH, Yao A, Chen YT, Hsu CN. FASTSNP: an always up-to-date and extendable service for SNP function analysis and prioritization. Nucleic Acids Res 2006; 34:W635–41-[PMID: 16845089].

40. Love-Gregory L, Sherva R, Sun L, Wasson J, Schappe T, Doria A, Rao DC, Hunt SC, Klein S, Neuman RJ, Permutt MA, Abumrad NA. Variants in the CD36 gene associate with the metabolic syndrome and high-density lipoprotein cholesterol. Hum Mol Genet 2008; 17:1695-704. [PMID: 18305138].

41. Love-Gregory L, Sherva R, Schappe T, Qi JS, McCrea J, Klein S, Connelly MA, Abumrad NA. Common CD36 SNPs reduce protein expression and may contribute to a protective

atherogenic profile. Hum Mol Genet 2011; 20:193-201. [PMID: 20935172].

42. She H, Nakazawa T, Matsubara A, Connolly E, Hisatomi T, Noda K, Kim I, Gragoudas ES, Miller JW. Photoreceptor protection after photodynamic therapy using dexamethasone in a rat model of choroidal neovascularization. Invest Ophthalmol Vis Sci 2008; 49:5008-14. [PMID: 18421085].

Articles are provided courtesy of Emory University and the Zhongshan Ophthalmic Center, Sun Yat-sen University, P.R. China. The print version of this article was created on 22 November 2012. This reflects all typographical corrections and errata to the article through that date. Details of any changes may be found in the online version of the article.

Clinical Ophthalmology

Dovepress
open access to scientific and medical research

Open Access Full Text Article

ORIGINAL RESEARCH

Effect of photodynamic therapy (PDT), posterior subtenon injection of triamcinolone acetonide with PDT, and intravitreal injection of ranibizumab with PDT for retinal angiomatous proliferation

Saya Nakano[1]
Shigeru Honda[1]
Hideyasu Oh[2]
Mihori Kita[2]
Akira Negi[1]

[1]Department of Surgery, Division of Ophthalmology, Kobe University Graduate School of Medicine, Kobe, [2]Department of Ophthalmology, Hyogo Prefectural Amagasaki Hospital, Amagasaki, Japan

Background: The purpose of this work was to compare the efficacy of photodynamic therapy (PDT) with or without posterior subtenon injections of triamcinolone acetonide (STA) or intravitreal injections of ranibizumab (IVR) for retinal angiomatous proliferation (RAP).

Methods: Thirty-seven eyes from 33 consecutive patients with RAP were treated by PDT monotherapy (Group 1), PDT combined with STA (Group 2), or PDT combined with IVR (Group 3). The best-corrected visual acuity, greatest linear dimension, central retinal thickness, and number of treatments were compared among the three groups.

Results: The change in mean best-corrected visual acuity (logMAR) at month 3, 6, and 12 after the initial treatment was better in Group 2 (−0.13, −0.23, and −0.21, respectively) and Group 3 (−0.018, 0.0028, and −0.0067, respectively) than in Group 1 (0.13, 0.19, and 0.23, respectively); Group 1 versus Group 2 was statistically significant ($P = 0.018$). The mean central retinal thickness was reduced from baseline in all groups, but the reduction amplitude was significantly greater in Group 2 than in Group 1 and Group 3. The mean number of treatments was significantly lower in Group 2 (1.1 ± 0.4) and Group 3 (1.5 ± 0.5) than in Group 1 (2.9 ± 0.9) in the 12 months after the initial treatment.

Conclusion: Treatment with STA + PDT may be an effective therapy for RAP lesions over 12 months of follow-up.

Keywords: retinal angiomatous proliferation, photodynamic therapy, triamcinolone acetonide, ranibizumab, combined therapy

Introduction

Age-related macular degeneration (AMD) is a leading cause of central vision loss in the elderly in industrialized countries.[1] The number of patients with AMD has increased remarkably over the years, and a further increase in patients with severe visual impairment due to AMD is anticipated.[2] Advanced AMD is clinically classified into atrophic AMD and exudative AMD. Exudative AMD is further classified into typical neovascular AMD, polypoidal choroidal vasculopathy, and retinal angiomatous proliferation (RAP).[1] These phenotypes are known to have different characteristics in their natural courses and their responses to interventions, such as photodynamic therapy (PDT) and antivascular endothelial growth factor (VEGF) therapy, although the reasons are unknown.[3–5] Several studies have reported a poor response to PDT monotherapy in patients with RAP lesions.[6,7] Hence, it is common to perform PDT combined with intravitreal injections of triamcinolone acetonide (IVT) or anti-VEGF

Correspondence: Shigeru Honda
Department of Surgery, Division of Ophthalmology, Kobe University Graduate School of Medicine, 7-5-2 Kusunoki-cho, Chuo-ku, Kobe 650-0017, Japan
Tel +81 78 382 6048
Fax +81 78 382 6059
Email sighonda@med.kobe-u.ac.jp

submit your manuscript | www.dovepress.com
Dovepress
http://dx.doi.org/10.2147/OPTH.S29718

therapy for RAP.[8,9] Several studies were conducted to address the comparative effectiveness between PDT monotherapy and the combination of PDT with IVT or anti-VEGF therapy against RAP lesions, but their conclusions were not consistent.[10,11] Rouvas et al reported that IVT + PDT was more effective than intravitreal ranibizumab (IVR) + PDT for RAP lesions.[10] In contrast, Saito et al reported that intravitreal bevacizumab + PDT was likely to be more effective than IVT + PDT in a Japanese RAP cohort.[11] This discrepancy might reflect the different anti-VEGF agents used in the two studies, so more replication studies are needed.

A posterior subtenon injection of triamcinolone acetonide (STA) is an alternative method to deliver triamcinolone acetonide to the posterior retina. Although IVT may cause an elevation in intraocular pressure and cataracts as complications,[12,13] STA might have fewer side effects in terms of inducing intraocular pressure elevation or cataracts than IVT because STA should act on the retina transsclerally and thus affect the lens and trabecular meshwork less than IVT.[14,15] However, to our knowledge, only a few published studies have compared the effectiveness of PDT combined with STA.[13] Therefore, in this study, we performed a comparative assessment between STA + PDT, IVR + PDT, and PDT alone in RAP patients.

Subjects and methods

This study was approved by the institutional review board of the Kobe University Graduate School of Medicine, and was conducted in accordance with the Declaration of Helsinki. Written informed consent was obtained from all subjects. All cases in this study were Japanese individuals recruited from the Department of Ophthalmology at Kobe University Hospital and Hyogo Prefectural Amagasaki Hospital in Japan.

This was a retrospective study of 37 eyes from 33 consecutive patients with RAP treated and followed up for more than 6 months. All patients received detailed ophthalmic examinations, including best-corrected visual acuity (BCVA) measurements, slit lamp biomicroscopy of their fundi, color fundus photography, fluorescein angiography, indocyanine green angiography, and optical coherence tomography. Visual acuities were determined using a Landolt C chart, and were converted to a logarithm of the minimum angle of resolution (logMAR) values for calculation. The diagnosis and staging of RAP was performed as previously described.[16] Patients with past histories of retinal vessel occlusion, uveitis, rhegmatogenous retinal detachment, or glaucoma were excluded.

Fourteen eyes from 12 consecutive patients recruited by May 2006 were treated by PDT monotherapy (Group 1), 12 eyes from 10 consecutive patients recruited from June 2006 to March 2009 were treated by PDT combined with STA (Group 2), and 11 eyes from 11 consecutive patients recruited thereafter were treated by PDT combined with IVR (Group 3). No patients in this study received previous therapy except for one patient in Group 2 who underwent PDT monotherapy 4 months earlier. For STA + PDT, a small incision was made in the lower temporal conjunctiva, and 20 mg of triamcinolone acetonide was injected retrobulbarly with a blunt needle 4–7 days before PDT. For IVR + PDT, 0.3 mg of ranibizumab was injected intravitreally with a 30-gauge needle 3–7 days before PDT. Patients were examined 3, 6, 9, and 12 months after the initial treatment, and were retreated if persistence or recurrence of intraretinal, subretinal, or subretinal pigment epithelium fluid, or any increase in retinal thickness was found by funduscopy or optical coherence tomography. The retreatment was done according to the same protocol as for the initial treatment.

For statistical analysis, we compared the gender, age, BCVA, greatest linear dimension, and central retinal thickness at baseline among the three groups. Changes in BCVA and central retinal thickness were then compared every 3 months until month 12 after the initial treatment. The number of treatments performed during the first 12 months after the initial treatment was compared among the groups. To evaluate the influence of STA on intraocular pressure, intraocular pressure values before and 2 weeks after STA were measured for the STA + PDT group. The Wilcoxon signed-rank test was performed to compare any two time points within the group and an analysis of variance was used to make a comparison between the groups. P values of 0.05 or less were considered to be statistically significant. StatView-J software (v 5.0; Abacus Corporation, Baltimore, MD) was used for statistical analyses.

Results

A summary of the data for the RAP patients is shown in Table 1. No differences were detected in baseline parameters between the three groups. The transition of values in mean BCVA (logMAR) and mean central retinal thickness are shown in Table 2. The change in mean BCVA at months 3, 6, and 12 after initial treatment was better in Group 2 (–0.13, –0.23, and –0.21) and Group 3 (–0.018, 0.0028, and –0.0067) than in Group 1 (0.13, 0.19, and 0.23); Group 1 versus Group 2 was statistically significant ($P = 0.018$, Figure 1). The mean BCVA was significantly better than baseline in Group 2 at 6 and 12 months after the initial treatment ($P = 0.012$ and 0.025, respectively). In contrast, the mean BCVA in Group 3 had deteriorated by 12 months after the initial treatment, although it was not significant ($P = 0.12$). The mean central retinal thickness was reduced from baseline after initial treatment in

Table 1 Baseline parameters of participants

	Group 1 (n 14)	Group 2 (n 12)	Group 3 (n 11)	P value
Gender (male/female)	11/1	6/4	4/7	0.022†
Age (mean ± SD, years)	82.3 ± 4.1	78.2 ± 5.7	80.3 ± 7.2	0.10*
RAP stage 1	1	3	3	0.61†
Stage 2	6	4	5	
Stage 3	7	5	3	
GLD (mean ± SD)	4737 ± 1704	3948 ± 1238	3291 ± 1418	0.10*
Baseline BCVA logMAR (mean ± SD)	0.82 ± 0.47	0.78 ± 0.55	0.84 ± 0.37	0.84*

Notes: Group 1, PDT monotherapy; Group 2, STA + PDT; Group 3, IVR + PDT; *Kruskal–Wallis test; †Chi-square test.
Abbreviations: GLD, greatest linear dimension; BCVA, best-corrected visual acuity; PDT, photodynamic therapy; STA, subtenon injection of triamcinolone acetonide; IVR, intravitreal injection of ranibizumab; SD, standard deviation.

all groups and the decrease was significant by 12 months in the STA + PDT and IVR + PDT groups (Figure 2). The reduction amplitude was significantly greater in Group 2 than in Group 1 and Group 3 ($P = 0.024$ and $P = 0.033$, respectively, for Group 1 versus Group 2 and Group 2 versus Group 3). In the cases followed up for more than 12 months after initial treatment, the mean number of treatments was significantly lower in Group 2 (1.1 ± 0.4, n = 12) and Group 3 (1.5 ± 0.5, n = 9) than in Group 1 (2.9 ± 0.9, n = 14) over 12 months after initial treatment (P 0.0001, $P = 0.0004$, and $P = 0.15$ for Group 1 versus Group 2, Group 1 versus Group 3 and Group 2 versus Group 3, respectively, Mann–Whitney test) (Figure 3). In Group 2, the mean intraocular pressure before and after STA was 13.8 ± 3.4 mmHg and 16.8 ± 6.1 mmHg, respectively, ($P = 0.18$, two-tailed paired t-test). No ocular or systemic complications were found or self-reported in the present cases.

Discussion

We compared the effects of PDT monotherapy, STA + PDT, and IVR + PDT in patients with RAP lesions, and found that the visual outcome was significantly better in those patients who underwent STA + PDT than in those treated with PDT monotherapy, although STA + PDT and IVR + PDT showed no significant difference in visual outcome. The mean number of treatments required per year was significantly lower in the STA + PDT and IVR + PDT groups than for the PDT monotherapy group. In addition, STA + PDT did not cause a significant elevation of intraocular pressure.

Currently, RAP is thought to be the most difficult subtype of exudative AMD to treat.[7] Because previous studies have demonstrated an insufficient effect of PDT monotherapy for RAP lesions,[6,7] most of the recent studies have focused on the effectiveness of PDT combined with IVT or anti-VEGF therapy.[8–11] However, few reports have evaluated the effects of STA + PDT for RAP. Montero et al reported that no better outcomes were observed in RAP patients treated with STA + PDT than in those treated with PDT monotherapy.[13] They administered 40 mg of triamcinolone acetonide immediately after PDT, which resulted in no significant difference in outcomes as compared with PDT monotherapy. However, we used 20 mg of triamcinolone acetonide 4–7 days before PDT, and obtained significantly better outcomes as compared with PDT monotherapy in RAP patients. This difference might be due to the insufficient time for transscleral diffusion of triamcinolone acetonide when it was applied after PDT.[14,15] Rouvas et al reported favorable outcomes for IVT + PDT when IVT was performed 7 ± 3 days before PDT.[10] The mechanism by which triamcinolone acetonide works to improve the outcome of PDT is still a matter of speculation. An inflammatory response and upregulation of VEGF have been reported after application of PDT.[17,18] Because triamcinolone acetonide has antiangiogenic, anti-inflammatory, and anti-VEGF effects,[19,20] the combination of PDT and triamcinolone acetonide may reduce the inflammatory response and upregulation of VEGF associated with choroidal neovascularization and PDT.

Table 2 Transition in best-corrected visual acuity and central retinal thickness of each group

	Group 1	Group 2	Group 3
BCVA (logMAR)			
Baseline	0.82 ± 0.47	0.78 ± 0.55	0.82 ± 0.38
3 months	0.95 ± 0.36	0.66 ± 0.37	0.80 ± 0.44
6 months	1.01 ± 0.31	0.56 ± 0.37*	0.82 ± 0.40
12 months	1.05 ± 0.32	0.57 ± 0.35*	0.81 ± 0.42
CRT (μm)			
Baseline	315 ± 93	358 ± 88	314 ± 102
3 months	268 ± 104	204 ± 72*	211 ± 51*
6 months	260 ± 93	202 ± 84*	223 ± 51*
12 months	263 ± 84	241 ± 74*	202 ± 46*

Notes: Group 1, PDT monotherapy; Group 2, STA + PDT; Group 3, IVR + PDT; *P 0.05 versus baseline.
Abbreviations: CRT, central retinal thickness; BCVA, best corrected visual acuity; PDT, photodynamic therapy; STA, subtenon injection of triamcinolone acetonide; IVR, intravitreal injection of ranibizumab.

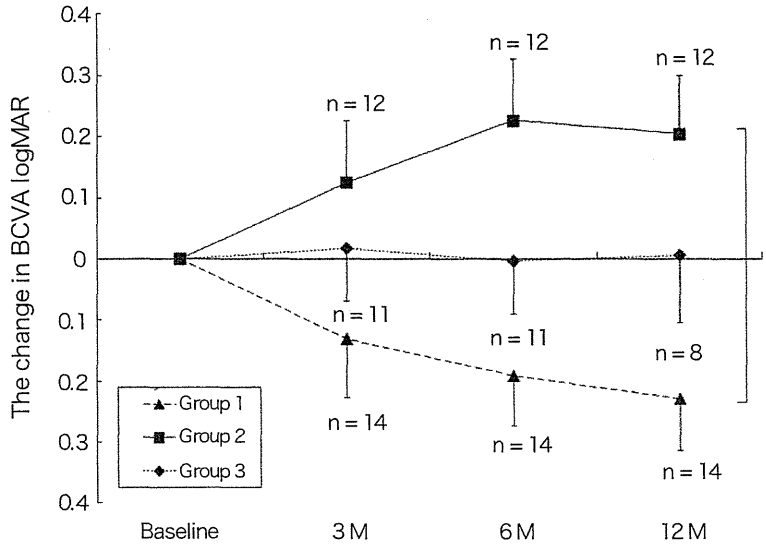

Figure 1 Changes in the BCVA of RAP patients after PDT, STA + PDT, and IVR + PDT. The BCVA was determined using the Landolt C chart, and is presented as decimal visual acuities. Triangles with dashed line: PDT (Group 1); squares with solid line: STA + PDT (Group 2); diamonds with dot line: IVR + PDT (Group 3).
Notes: Values represent mean ± SEM; *P 0.05 compared to baseline; **P 0.05 between Group 1 and Group 2.
Abbreviations: BCVA, best corrected visual acuity; IVR, intravitreal injections of ranibizumab; RAP, retinal angiomatous proliferation; PDT, photodynamic therapy, STA, subtenon injections of triamcinolone acetonide.

The significantly greater central retinal thickness reduction after STA + PDT than after IVR + PDT in the present study might reflect a difference in anti-inflammatory and anti-VEGF effects between STA and IVR, which was possibly associated with the better outcome, although not significant, in the post-treatment BCVA for the STA + PDT group than for the IVR + PDT group. Although we performed IVR 3–7 days before PDT, the timing of IVR might be too early because Debefe et al reported that ranibizumab should be administered within 24 hours after PDT in accordance with their experimental results.[21] A recent report showed favorable visual outcomes after IVR + PDT when PDT was performed 1–2 days after IVR.[22] In addition, unlike previous reports, we did not add two extra monthly IVR after PDT in Group 3 to save treatment costs, which might reduce the effect of IVR + PDT. However, the change in logMAR BCVA in Group 3 was almost equivalent to that of the previous report (0.02 between baseline and at least 6 months after the first therapy) performing three IVR + one PDT as an initial treatment.[10] There is another possibility that the effects of

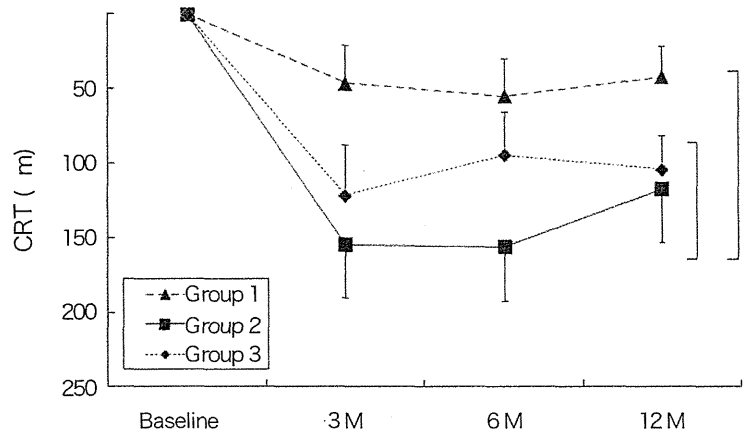

Figure 2 Changes in the CRT of RAP patients after PDT, STA + PDT, and IVR + PDT. Triangles with dashed line: PDT (Group 1); squares with solid line: STA + PDT (Group 2); diamonds with dot line: IVR + PDT (Group 3).
Notes: Values represent mean ± SEM. *P 0.05. **P 0.05 between Group 1 and Group 2, or between Group 2 and Group 3.
Abbreviations: CRT, central retinal thickness; IVR, intravitreal injections of ranibizumab; RAP, retinal angiomatous proliferation; PDT, photodynamic therapy, STA, subtenon injections of triamcinolone acetonide.

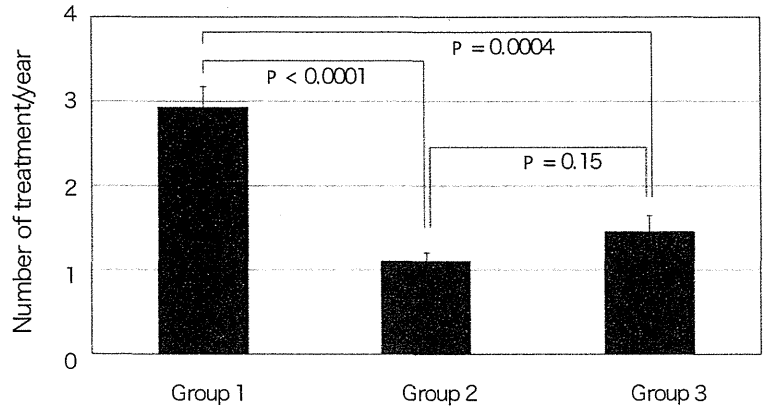

Figure 3 Number of treatments performed in 12 months.
Note: Values represent mean + SEM.

STA remained for several months after PDT and inhibited regrowth of neovascular tracts, reducing the number of treatments required to suppress the RAP lesions, and thus resulted in reduced cumulative retinal damage caused by PDT. Because a single STA is thought to have antiangiogenic and anti-inflammatory effects lasting up to 3 months[23] while a single dose of IVR can work for a month, STA + PDT might have an advantage to suppress the RAP lesion longer than IVR + PDT. Conversely, IVR + PDT may necessitate some additional IVR during follow-up period.

Our results showed that the best mean BCVA was obtained at 6 months after the initial STA + PDT, but this was reduced by 12 months, mainly due to reactivation of RAP lesions in some cases. It is interesting that a reactivation of RAP lesions at 6 months after treatment was previously reported in cases treated with IVT + PDT.[24] A previous review article mentioned that the best improvement in BCVA was achieved at 6 months after initial PDT + IVT, and that the effects faded by 12 months, with a high incidence of cataracts.[9] However, in our study, no patient in the STA + PDT group showed any progression of cataracts during the follow-up period. In addition, the incidence of intraocular pressure elevation was reported less often with STA than with IVT.[25]

Currently, many treatment procedures are being tested and compared to establish the best strategy for treating RAP lesions. Among them, anti-VEGF therapy is the most investigated modality which could be applied alone[26,27] or combined with PDT.[10,11,28] However, IVR + PDT is likely to be a very expensive therapy and intravitreal bevacizumab + PDT is not possible without off-label use of bevacizumab under current circumstances. If STA + PDT showed similar or better outcomes to PDT+ anti-VEGF therapy or anti-VEGF monotherapy, there is a greater cost-effectiveness for patients. In fact, the improvement in BCVA (–0.22 ± 0.34 logMAR units) with STA + PDT in this study was almost equivalent to the average of previous reports (–0.17 ± 0.12 logMAR units) with anti-VEGF monotherapy.[9,29]

The major limitations of the present study were its non-randomized and retrospective nature and the small number of subjects. Hence, it is important to evaluate the results of a randomized controlled trial for STA + PDT with a larger number of subjects to determine the efficacy of this therapy, particularly against RAP. Therefore, further investigation will be needed to determine the correct interventions for RAP.

In conclusion, STA + PDT may be an effective therapy for RAP lesions during the first 12 months after treatment, although the effects need to be further evaluated.

Acknowledgments

This study was supported by a grant-in aid (23592567) from the Ministry of Education, Science, and Culture, Tokyo, Japan (SH), and by a grant from the Takeda Science Foundation (SH).

Disclosure

No authors have any financial or conflicting interests to disclose in this work.

References

1. Cook HL, Patel PJ, Tufail A. Age-related macular degeneration: diagnosis and management. *Br Med Bull*. 2008;85:127–149.
2. Rein DB, Wittenborn JS, Zhang X, et al. Forecasting age-related macular degeneration through the year 2050: the potential impact of new treatments. *Arch Ophthalmol*. 2009;127:533–540.
3. Honda S, Kurimoto Y, Kagotani Y, et al. Photodynamic therapy for typical age-related macular degeneration and polypoidal choroidal vasculopathy: a 30-month multicenter study in Hyogo, Japan. *Jpn J Ophthalmol*. 2009;53:593–597.
4. Honda S, Imai H, Yamashiro K, et al. Comparative assessment of photodynamic therapy for typical age-related macular degeneration and polypoidal choroidal vasculopathy: a multicenter study in Hyogo prefecture, Japan. *Ophthalmologica*. 2009;223:333–338.

5. Lim JY, Lee SY, Kim JG, Lee JY, Chung H, Yoon YH. Intravitreal bevacizumab alone versus in combination with photodynamic therapy for the treatment of neovascular maculopathy in patients aged 50 years or older: 1-year results of a prospective clinical study. *Acta Ophthalmol.* 2010. [Epub ahead of print.]
6. Boscia F, Furino C, Sborgia L, Reibaldi M, Sborgia C. Photodynamic therapy for retinal angiomatous proliferations and pigment epithelium detachment. *Am J Ophthalmol.* 2004;138: 1077–1079.
7. Boscia F, Parodi MB, Furino C, Reibaldi M, Sborgia C. Photodynamic therapy with verteporfin for retinal angiomatous proliferation. *Graefes Arch Clin Exp Ophthalmol.* 2006;244:1224–1232.
8. Krebs I, Krepler K, Stolba U, Goll A, Binder S. Retinal angiomatous proliferation: combined therapy of intravitreal triamcinolone acetonide and PDT versus PDT alone. *Graefes Arch Clin Exp Ophthalmol.* 2008;246:237–243.
9. Gupta B, Jyothi S, Sivaprasad S. Current treatment options for retinal angiomatous proliferans (RAP). *Br J Ophthalmol.* 2010;94:672–677.
10. Rouvas AA, Papakostas TD, Vavvas D, et al. Intravitreal ranibizumab, intravitreal ranibizumab with PDT, and intravitreal triamcinolone with PDT for the treatment of retinal angiomatous proliferation: a prospective study. *Retina.* 2009;29:536–544.
11. Saito M, Shiragami C, Shiraga F, Kano M, Iida T. Comparison of intravitreal triamcinolone acetonide with photodynamic therapy and intravitreal bevacizumab with photodynamic therapy for retinal angiomatous proliferation. *Am J Ophthalmol.* 2010;149: 472–481.
12. Ruiz-Moreno JM, Montero JA, Barile S, Zarbin MA. Photodynamic therapy and high-dose intravitreal triamcinolone to treat exudative age-related macular degeneration: 1-year outcome. *Retina.* 2006;26:602–612.
13. Monterò JA, Ruiz-Moreno JM, Sanabria MR, Fernandez-Munoz M. Efficacy of intravitreal and periocular triamcinolone associated with photodynamic therapy for treatment of retinal angiomatous proliferation. *Br J Ophthalmol.* 2009;93:166–170.
14. Mora P, Eperon S, Felt-Baeyens O, et al. Trans-scleral diffusion of triamcinolone acetonide. *Curr Eye Res.* 2005;30:355–361.
15. Lee SJ, Kim ES, Geroski DH, McCarey BE, Edelhauser HF. Pharmacokinetics of intraocular drug delivery of Oregon green 488-labeled triamcinolone by subtenon injection using ocular fluorophotometry in rabbit eyes. *Invest Ophthalmol Vis Sci.* 2008;49: 4506–4514.
16. Yannuzzi LA, Negrao S, Iida T, et al. Retinal angiomatous proliferation in age-related macular degeneration. *Retina.* 2001;21:416–434.
17. Tatar O, Adam A, Shinoda K, et al. Influence of verteporfin photodynamic therapy on inflammation in human choroidal neovascular membranes secondary to age-related macular degeneration. *Retina.* 2007;27:713–723.
18. Tatar O, Adam A, Shinoda K, et al. Expression of VEGF and PEDF in choroidal neovascular membranes following verteporfin photodynamic therapy. *Am J Ophthalmol.* 2006;142:95–104.
19. Penfold PL, Wen L, Madigan MC, King NJ, Provis JM. Modulation of permeability and adhesion molecule expression by human choroidal endothelial cells. *Invest Ophthalmol Vis Sci.* 2002;43:3125–3130.
20. Hori Y, Hu DE, Yasui K, Smither RL, Gresham GA, Fan TP. Differential effects of angiostatic steroids and dexamethasone on angiogenesis and cytokine levels in rat sponge implants. *Br J Pharmacol.* 1996;118:1584–1591.
21. Debefve E, Pegaz B, Ballini JP, van den Bergh H. Combination therapy using verteporfin and ranibizumab; optimizing the timing in the CAM model. *Photochem Photobiol.* 2009;85:1400–1408.
22. Saito M, Iida T, Kano M. Combined intravitreal ranibizumab and photodynamic therapy for retinal angiomatous proliferation. *Am J Ophthalmol.* 2011. [Epub ahead of print].
23. Shen L, You Y, Sun S, Chen Y, Qu J, Cheng L. Intraocular and systemic pharmacokinetics of triamcinolone acetonide after a single 40-mg posterior subtenon application. *Ophthalmology.* 2010;117:2365–2371.
24. Reche-Frutos J, Calvo-Gonzalez C, Donate-Lopez J, et al. Retinal angiomatous proliferation reactivation 6 months after high-dose intravitreal acetonide triamcinolone and photodynamic therapy. *Eur J Ophthalmol.* 2007;17:979–982.
25. Hirano Y, Ito T, Nozaki M, et al. Intraocular pressure elevation following triamcinolone acetonide administration as related to administration routes. *Jpn J Ophthalmol.* 2009;53:519–522.
26. Konstantinidis L, Mameletzi E, Mantel I, Pournaras JA, Zografos L, Ambresin A. Intravitreal ranibizumab (Lucentis) in the treatment of retinal angiomatous proliferation (RAP). *Graefes Arch Clin Exp Ophthalmol.* 2009;247:1165–1171.
27. Hemeida TS, Keane PA, Dustin L, Sadda SR, Fawzi AA. Long-term visual and anatomical outcomes following anti-VEGF monotherapy for retinal angiomatous proliferation. *Br J Ophthalmol.* 2010;94:701–705.
28. Viola F, Mapelli C, Villani E, et al. Sequential combined treatment with intravitreal bevacizumab and photodynamic therapy for retinal angiomatous proliferation. *Eye (Lond).* 2010;24:1344–1351.
29. Parodi MB, Iacono P, Menchini F, et al. Intravitreal bevacizumab versus ranibizumab for the treatment of retinal angiomatous proliferation. *Acta Ophthalmol.* 2011. [Epub ahead of print].

Montage Images of Spectral-Domain Optical Coherence Tomography in Eyes with Idiopathic Macular Holes

Keisuke Mori, MD, PhD,[1] Junji Kanno, OP,[1] Peter L. Gehlbach, MD, PhD,[2] Shin Yoneya, MD, PhD[1]

Purpose: To describe the morphologic and anatomic relationships at the vitreoretinal interface, from the macula into the periphery, in patients with idiopathic macular hole. Montaged images of posterior and peripheral spectral-domain (SD) optical coherence tomography (OCT) studies were used to describe the anatomic vitreoretinal relationships.

Design: Prospective, consecutive, observational case series.

Participants: Forty-six eyes of thirty-six consecutive patients with idiopathic macular hole and their fellow eyes.

Methods: Montage images of 4 radial OCT scans (horizontal, vertical, and 2 oblique scans) through the fovea were obtained in each case.

Main Outcome Measures: Montage SD OCT images.

Results: In fellow eyes, potential precursor changes to macular hole revealed shallow perifoveal vitreous separation that extends peripherally toward the equator. Two distinct configurations were noted at the posterior vitreous face; eyes without holes had a smooth curvature, whereas eyes with holes were more likely to have wavy, folded, or scalloped vitreous surfaces. At the onset of separation, most posterior vitreous cortex had a smooth curvature, but posterior vitreous folds increased with progressive separation. Also notable were zones of double-layered retinoschisis in regions of adherent posterior vitreous. Resulting granular hyperreflection in the peripheral vitreous was detectable in 50% to 60% of stage 1 or 2 holes but in only 33% of stage 3 or 4 holes.

Conclusions: The SD OCT montages taken at serial stages of idiopathic macular holes document distinct configurations of the posterior vitreous face, granular hyperreflection in the peripheral vitreous, and areas of peripheral retinoschisis. Montaging SD OCT images provides novel cross-sectional images of the vitreoretinal interface that may have broader application.

Financial Disclosure(s): The author(s) have no proprietary or commercial interest in any materials discussed in this article. *Ophthalmology 2012;119:2600–2608 © 2012 by the American Academy of Ophthalmology.*

Current concepts as to the pathophysiologic features of idiopathic macular hole have evolved with greater understanding of the vitreoretinal interface. Central to this understanding is that vitreomacular traction is integral to the development and progression of a full-thickness macular hole. Gass[1,2] proposed a hypothesis of macular hole formation based primarily on biomicroscopic observations that suggested contraction of perifoveal cortical vitreous with resulting tangential traction. Based largely on these observations, removal of posterior vitreous cortex in patients with impending and full-thickness macular holes has resulted in favorable therapeutic outcomes.[3–5]

Optical coherence tomography (OCT) is capable of providing high-resolution tomographic images of the posterior vitreous, retina, and choroid.[6] Hee et al[7] demonstrated that OCT is able to detect small separations of the posterior vitreous from the retina in unaffected fellow eyes of patients with macular holes. In prior work, the authors' group demonstrated dome-shaped perifoveal vitreous detachment around the macular hole in its early stages.[8,9] Gaudric et al[10] also demonstrated convex perifoveal detachment of posterior hyaloid in fellow eyes of patients with macular holes. These OCT findings suggest a modified theory of macular hole formation that more strongly implicates anteroposterior traction resulting from age-related perifoveal vitreous detachment, as opposed to tangential traction secondary to contraction of cortical vitreous. However, these OCT observations previously were limited to the macular region. The present study examined the vitreoretinal interface in the periphery and provided further insights into the basic pathophysiologic features of macular hole development and progression. Recent developments in spectral-domain (SD) OCT imaging have increased the axial resolution, signal-to-noise ratio, scan rate, and scan length resulting in dramatic improvements in the visualization of the vitreoretinal interface and posterior vitreous cortex. Human peripheral retinal images were obtained successfully with SD OCT, and normative data are presented describing regional differences and aging changes in the macula and more peripheral retina (Omata H, et al. Normative values for foveolar, macular and peripheral retinal thickness by spectral-domain optical tomography. Paper presented at: ARVO Annual Meeting, May 3, 2010; Fort Lauderdale, FL). In the present study, montages of SD OCT images were created that delineate the posterior vitreous cortex and the vitreoretinal interface from the macula to approximately the equator. The montaged

ISSN 0161-6420/12/$–see front matter
http://dx.doi.org/10.1016/j.ophtha.2012.06.027

images clearly demonstrated 2 distinct configurations of the posterior vitreous cortex that correlated with stage of macular hole development. The patterns are suggestive of potential tractional force development at the vitreoretinal interface in the evolving macular hole.

Patients and Methods

Patients and Study Design

This was a prospective, consecutive, observational case series. Forty-six consecutive eyes of 36 patients with a clinical diagnosis of idiopathic macular hole, but without other ocular complications were enrolled into this study. All investigations adhered to the tenets of the Declaration of Helsinki. This study was approved by the institutional review board of the Saitama Medical University. The composition of the patient population was 20 females and 16 males, ranging in age from 46 to 79 years (mean±standard deviation, 65.1±7.4 years). All patients gave informed consent to participate in this study. All patients were examined by indirect ophthalmoscopy, contact lens slit-lamp biomicroscopic examination, fundus photography, visual acuity testing, and the Watzke-Allen test. Data included identification of the study eye, date of onset of symptoms, refraction, best-corrected visual acuity, fellow eye diagnosis, classification of the macular hole, description of any vitreous (traction), and the montaged SD OCT images.

The diagnosis and classification of macular holes was based on slit-lamp biomicroscopic examination using the criteria described by Gass,[1,2] and these were supported by OCT findings. The samples consist of 4 eyes with a stage 1A hole, 2 eyes with a stage 1B hole, 10 eyes with a stage 2 hole, 12 eyes with a stage 3 hole, and 12 eyes with a stage 4 hole (Table 1). In addition, with respect to the clinically normal fellow eyes, 6 fellow eyes with perifoveal posterior vitreous detachment with still normal foveal structure were examined in this study. Fellow eyes of patients with existing macular holes previously were noted to have precursor findings (so-called stage 0 holes[11,12]) and do have a higher rate of macular hole formation than eyes of patients without macular holes.

Montage Images of Spectral-Domain Optical Coherence Tomography

The OCT images were obtained through a dilated pupil by a trained examiner (J.K.) without prior knowledge of clinical retinal findings. All OCT examinations were performed using SD OCT (Spectralis; Heidelberg Engineering, Vista, CA). Standardized horizontal, vertical, and 2 oblique (supertemporal to inferonasal and supranasal to inferotemporal) vitreoretinal sections through the macular hole were collected for each patient. To examine the morphologic features of the entire posterior vitreous cortex and the vitreoretinal interface, wide-angle montage images of OCT from the macula to the periphery (approximately the equator) were obtained. Montage images were composed using picture editing software (Photoshop version 5.5; Adobe, San Jose, CA).

Results

The appearance and configuration of the posterior vitreous in fellow eyes and macular hole eyes grouped by Gass stages are described herein. A series of images is presented and, in most examples, there are 1 of 2 typical patterns, termed *smooth* (Figs 1 and 2) and *wavy or scalloped* (Figs 3, 4, and 5).

Fellow Eyes with Shallow Perifoveal Vitreous Separation (Stage 0 Macular Holes)

In an attempt to examine precursor findings to a stage 1 hole, 6 fellow eyes with perifoveal posterior vitreous detachment were examined. There were no obvious alterations in foveal or macular structure. Perifoveal retina is the thickest region of the retina. Both retinal and choroidal thickness decreases toward the periphery.

In all 6 eyes, posterior vitreous was delineated clearly in montage images of SD OCT. Even in the fellow eye, shallow perifoveal vitreous separation was not limited to the macular region, but extended toward the equator. In 5 of 6 eyes (83%), posterior vitreous cortex had a smooth curvature and was adherent to the disc, fovea, and peripheral retina. The remaining eye (17%) had a wavy posterior vitreous that was different than that of the other 5 eyes and was consistent with release of vitreoretinal adhesion. Also noted was a granular hyperreflective zone in the peripheral vitreous in 4 of 6 eyes (67%) (Fig 1).

Stage 1 Macular Holes

The 4 eyes with a stage 1A macular hole demonstrated foveal splitting in the outer nuclear layer that was associated with anteroposterior vitreous traction (Fig 2). In 2 eyes with a stage 1B macular hole, there was an intraretinal foveal splitting extending to the outer retina (Fig 3). In 3 of 6 eyes (50%) with a stage 1 hole (50% of stage 1A holes and 50% of stage 1B holes), a shallow perifoveal vitreous separation with a smooth contour similar to that shown in stage 0 holes was present. The remaining eyes had a posterior vitreous cortex with a wavy or scalloped contour. There

Table 1. Macular Hole Stages and Incidences of Optical Coherence Tomography Findings

Stages	No.	Granular Hyperreflection in the Peripheral Vitreous	Peripheral Retinoschisis	Wavy Posterior Vitreous Fold
Fellow Eye	6	4/6 (67)	1/6 (17)	1/6 (17)
1	6	3/6 (50)	3/6 (50)	3/6 (50)
1A	4	2/4 (50)	1/4 (25)	2/4 (50)
1B	2	1/2 (50)	2/2 (100)	1/2 (50)
2	10	6/10 (60)	0/10 (0)	8/10 (80)
3	12	4/12 (33)	0/12 (0)	12/12 (100)
4	12	1/3 (33)*	0/3 (0)*	3/3 (100)*
Total	46	18/37 (49)	4/37 (11)	27/37 (73)

Data are expressed as the number of subject/group (% of entire group).
*Nine cases were excluded because the posterior vitreous shifted anteriorly outside of the range of observations.

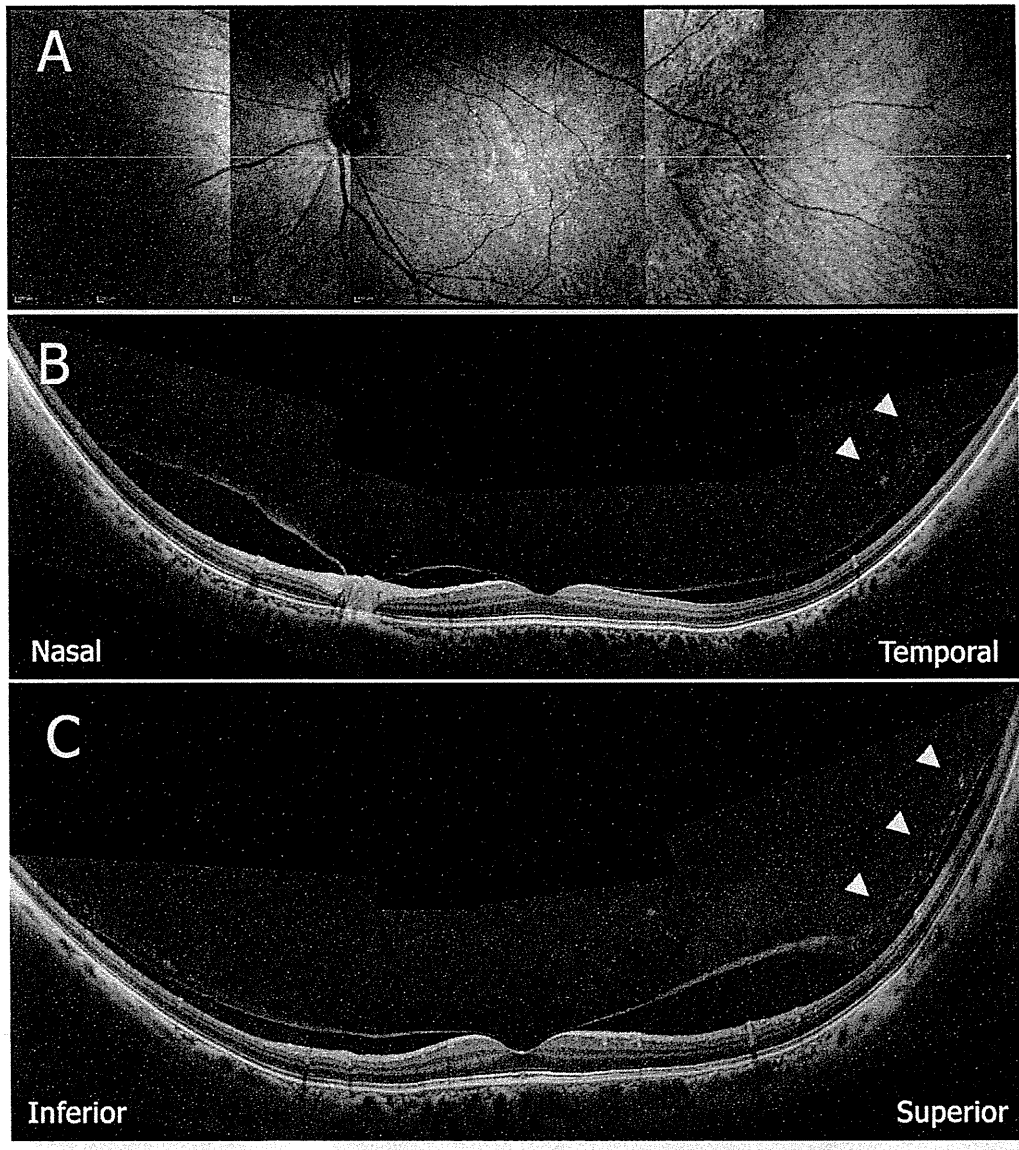

Figure 1. Montage images of (**A**) an infrared fundus photograph and (**B**) horizontal and (**C**) vertical vitreous–retina–choroid cross-sections in a fellow eye with perifoveal posterior vitreous detachment. A long transverse arrow in (**A**) corresponds to the scanning line for the vertical cross-section in (**B**). There is no obvious alteration in the retinal structure. A shallow perifoveal vitreous separation expands toward the equator over the vascular arcade. Posterior vitreous draws a smooth curvature adherent to the disc, fovea, and peripheral retina. Note the granular hyperreflection in the peripheral vitreous (arrowheads).

was also double-layered retinoschisis (intraretinal splitting) versus intraretinal fluid collection of the peripheral retina to which there was adherent to posterior vitreous cortex (Figs 2F and 3E). These zones of double-layered retinoschisis were detectable in 1 of 6 fellow eyes (17%) with a stage 0 hole and in 3 of 6 eyes (50%) with a stage 1 hole (25% of stage 1A holes and 100% of stage 1B holes), but not in eyes with stage 2 through 4 holes. Each peripheral retinoschisis was located in the superior, supranasal, or supertemporal quadrants, or a combination thereof. There were zones containing granular hyperreflective points in the peripheral vitreous in 3 of 6 eyes (50%). These hyperreflective granules were not evident in the macular regions.

Stage 2 Macular Holes

In stage 2 macular holes, 8 of 10 eyes (80%) had wavy or scalloped posterior vitreous folds along the curvature of vitreous detachment. Typically vitreous separation extended farther in the superior and temporal quadrants than in inferior and nasal quadrants. Although posterior vitreous of the smooth curvature configuration (without scalloping) formed a shallow acute angle with the peripheral retina, a wavy line-shaped posterior vitreous (with scalloping) was attached to the peripheral retina at a greater angle of insertion. This was most notable in the superior and temporal quadrants. Posterior vitreous cortex had a wavy or scalloped configuration in these quadrants. Granular hyperreflection in the peripheral vitreous was evident in 6 of 10 eyes (60%). The peripheral retinoschisis was not detectable in any of the examined eyes with stage 2 holes.

Stage 3 or 4 Macular Holes

In 9 of 12 eyes with a stage 4 macular hole, the posterior vitreous face was separated anteriorly and was too peripheral to image. In all 15 eyes with stage 3 or 4 macular holes with observable

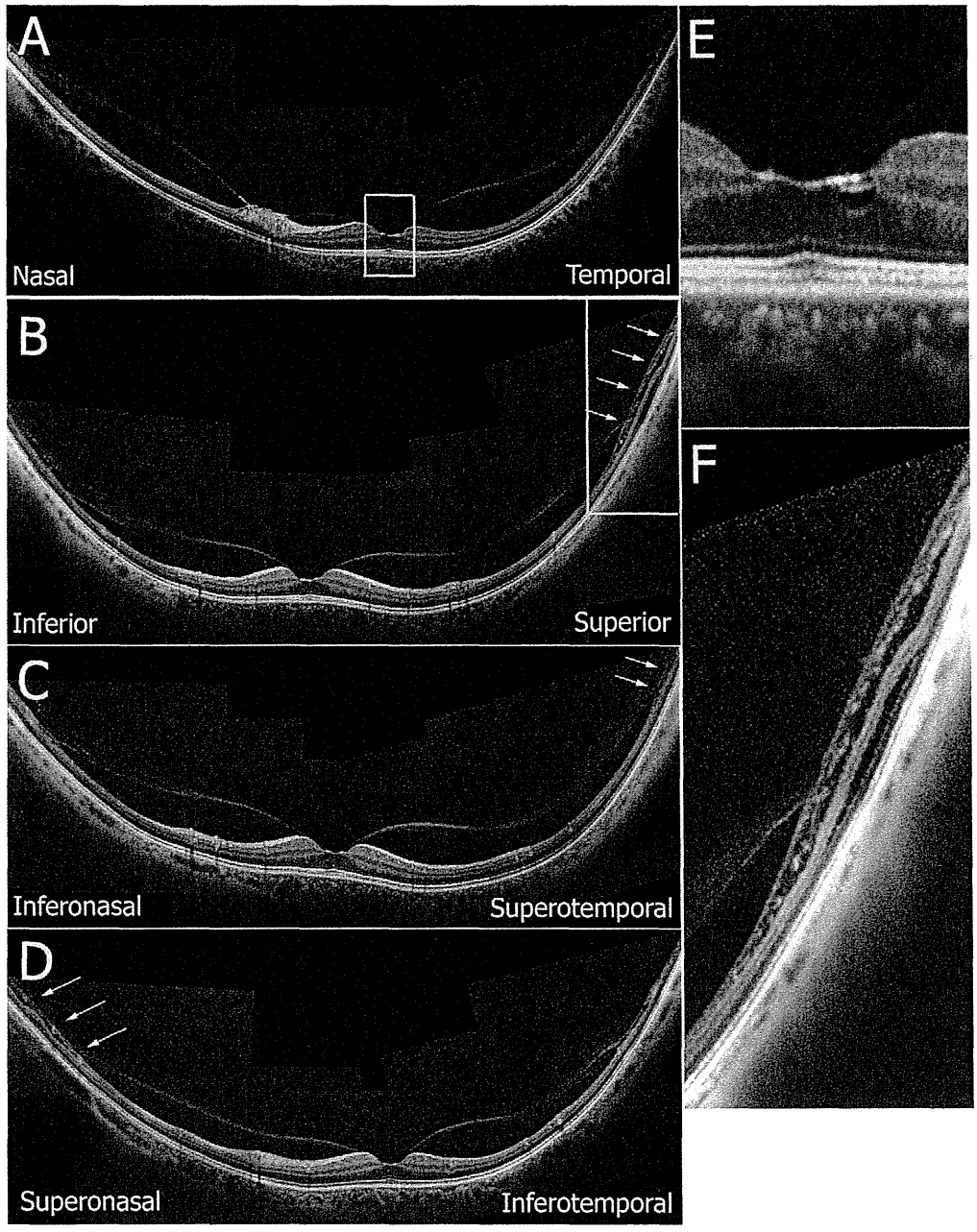

Figure 2. Montage images of (**A**) horizontal, (**B**) vertical, (**C**) oblique (inferonasal to supertemporal), and (**D**) oblique (supranasal to inferotemporal) vitreous–retina–choroid cross-sections in an eye with an early stage 1A macular hole. A highly magnified image of an inset in (**A**) is shown in (**E**) and that of an inset in (**B**) is shown in (**F**). (**E**) There is mild foveal splitting in the superficial outer nuclear layer. A shallow perifoveal vitreous separation expands toward the equator. There is a smooth curvature of the vitreous face adherent to the disc, fovea, and peripheral retina similar to that of the fellow eye (Fig 1). (**F**) Note the double-layered retinoschisis (intraretinal splitting) in the inner and outer plexiform layers of the peripheral retina adherent to posterior vitreous. These zones of retinoschisis were evident in the superior, supertemporal, and supranasal quadrants (arrows in B, C, D).

posterior vitreous, 100% had wavy posterior vitreous folds. Wavy folds were visible throughout the entire separated posterior vitreous cortex. The folds were thicker and wider morphologically than those in the earlier stage macular holes (Fig 5). The incidence of a wavy as opposed to smooth posterior vitreous increased with progression of the stage of macular hole (Table 1). The granular hyperreflection in the peripheral vitreous was evident in 5 of 15 eyes (33%) with stage 3 and 4 holes (33% with a stage 3 hole and 33% with a stage 4 hole). Peripheral retinoschisis was not detectable in any eyes with a stage 3 or 4 hole.

Discussion

This study assembled montaged OCT images of the posterior vitreous, retina, and choroid that extended from the macula to the periphery and examined the morphologic relationships between these structures during development and progression of idiopathic macular holes. The posterior vitreous cortex was delineated clearly in all eyes except those with very anterior vitreous detachment. This finding

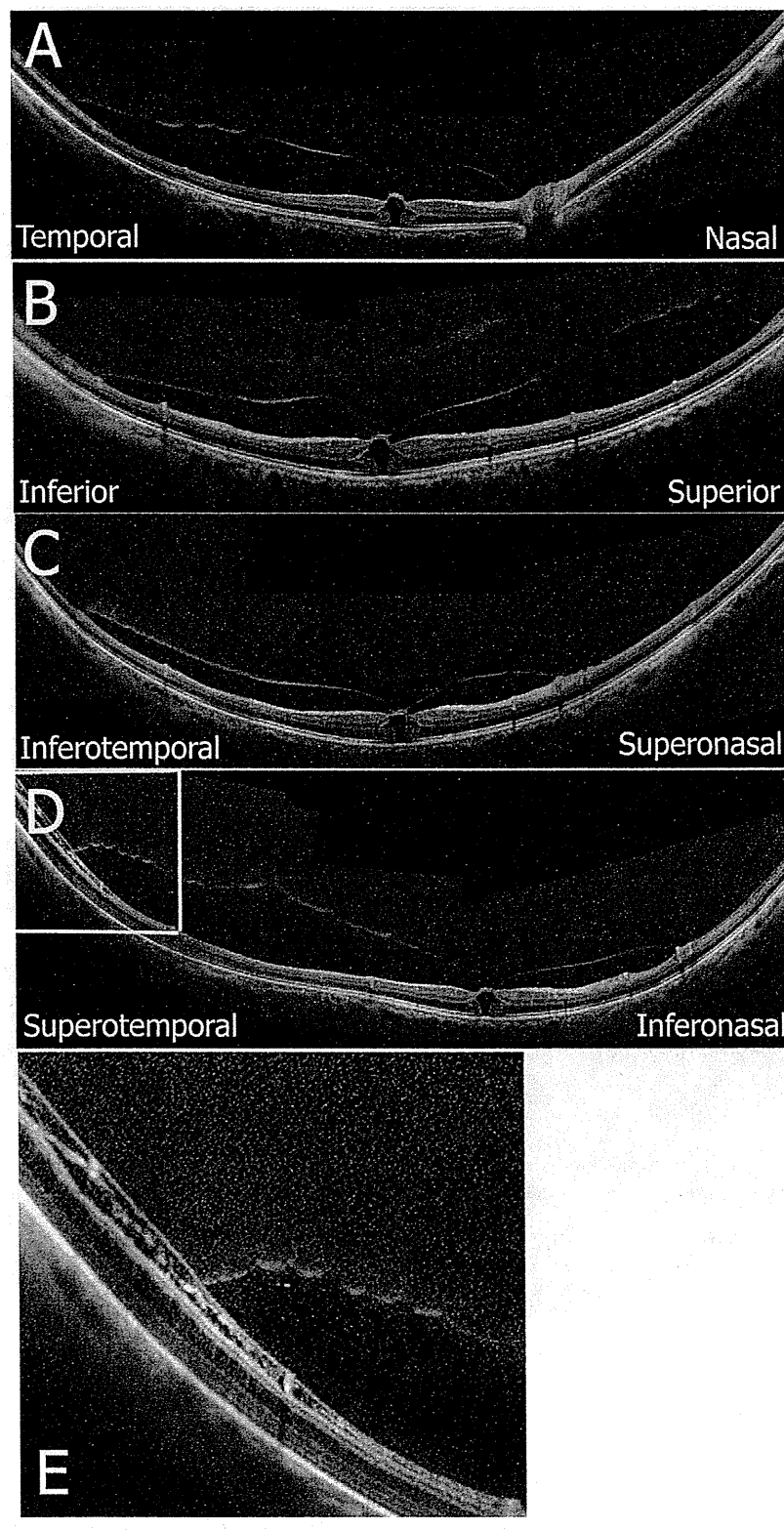

Figure 3. Montage images of (**A**) horizontal, (**B**) vertical, (**C**) oblique (inferotemporal to supranasal), and (**D**) oblique (supertemporal to inferonasal) vitreous–retina–choroid cross-sectional images in an eye with a stage 1B macular hole. A highly magnified image of an inset in (**D**) is shown in (**E**). There is intraretinal foveal splitting extending to the outer retina. Vitreous separation extends toward the equator. The vitreous face has a wavy surface with a more scalloped configuration than the smooth curvature seen in Figures 1 and 2. Although posterior vitreous of the smooth curvature configuration forms a shallow, acute angle with the peripheral retina, the wavy line configuration shown here shows a steep insertion angle at the point of peripheral adhesion. Typically, vitreous separation extends more peripherally in the superior and temporal quadrants than in the inferior and nasal quadrants. (**E**) Note the double-layered retinoschisis in the inner and outer plexiform layers in a supertemporal quadrant.

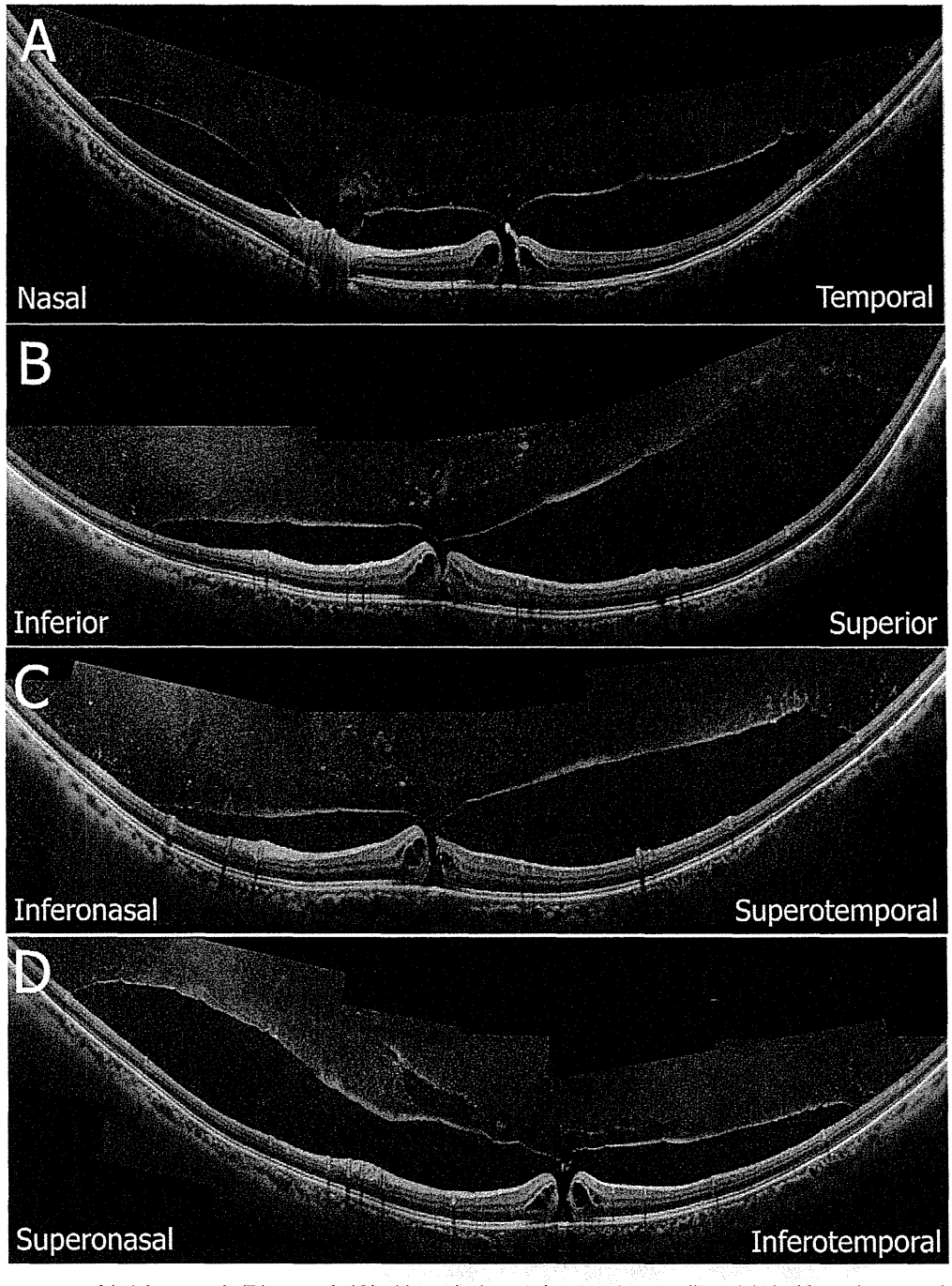

Figure 4. Montage images of (**A**) horizontal, (**B**) vertical, (**C**) oblique (inferonasal to supertemporal), and (**D**) oblique (supranasal to inferotemporal) vitreous–retina–choroid cross-sectional images in an eye with a stage 2 macular hole. (**A**) The posterior vitreous face remains attached to the roof of the hole. The posterior vitreous is not drawn taught into a straight line, especially in the periphery of the superior and temporal quadrants.

was noted only in eyes with stage 4 holes. Eyes predisposed to macular hole formation were examined by examining fellow eyes in patients with a macular hole, and shallow perifoveal vitreous separation was identified that was not limited to the macular region, but rather extended toward the equator beyond the vascular arcades. There were 2 distinct patterns observed in images of the separated posterior vitreous face. At the time of initiation of posterior vitreous detachment, most posterior vitreous cortex had a smooth curvature to the vitreous face with attachment to the disc, fovea, and peripheral retina. The development of the second hyaloid face configuration, wavy or scalloped posterior vitreous folds, increased in association with macular hole progression. In advanced staged holes (stage 3 or 4), these folds were visible throughout the posterior vitreous face and were thicker and wider than those observed in early stage macular holes. The notable finding of wavy posterior vitreous folds at the vitreous face may support a hypothesis

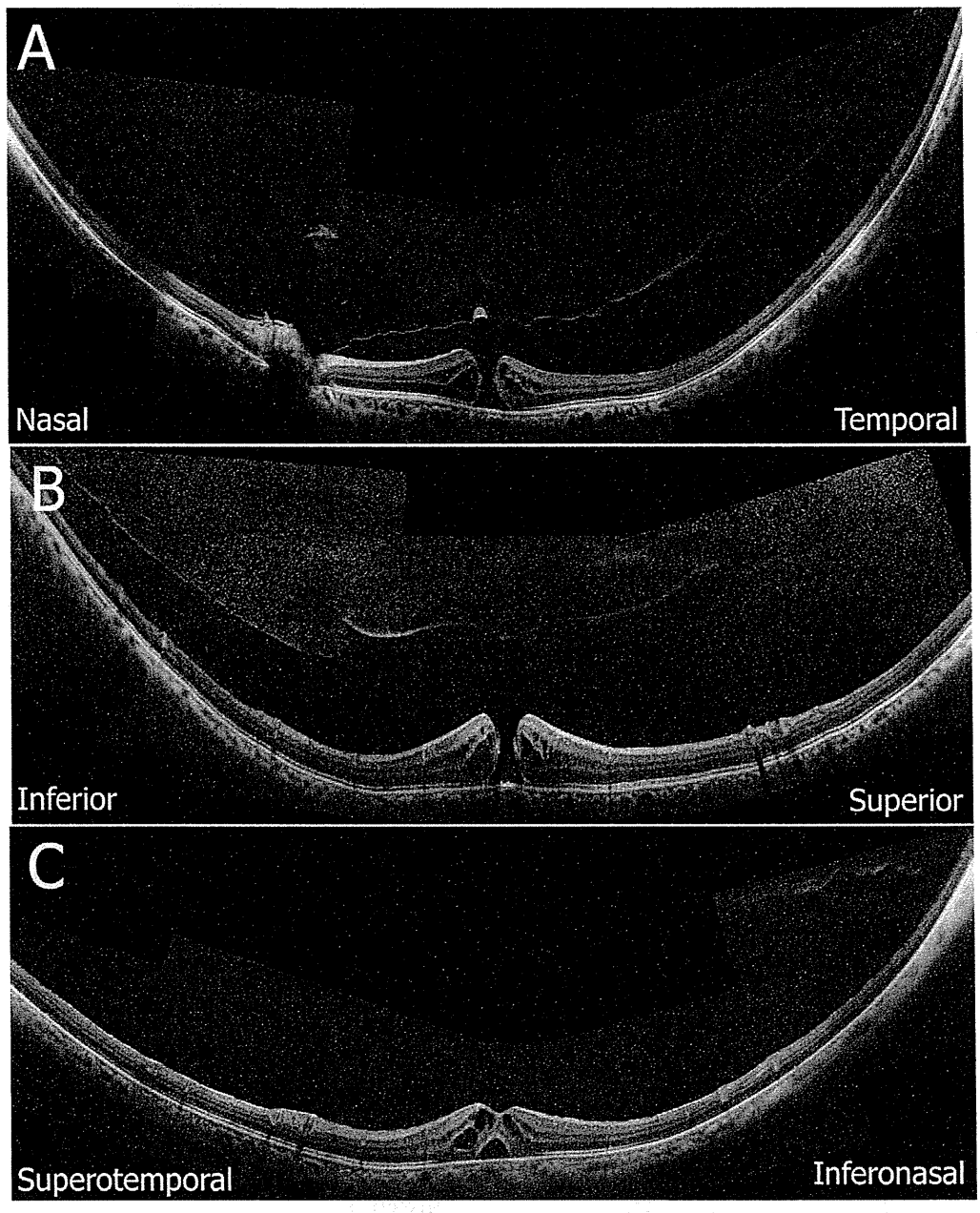

Figure 5. Montage images of (A) horizontal and (B) vertical vitreous–retina–choroid cross-sections in an eye with a stage 3 macular hole and (C) an oblique scan with a stage 4 hole. (B) The posterior vitreous face is not visible in the superior quadrant in this stage 3 hole because vitreous separation extends anteriorly beyond the field of image acquisition for the optical coherence tomography image. Wavy posterior vitreous folds are visible throughout posterior vitreous. (C) In a stage 4 hole, posterior vitreous is not at all or only partially visible.

that the posterior vitreous becomes loose rather than taught during the course of progression of macular holes. This finding also supports the hypothesis that the anteroposterior tractional forces at the fovea are generated mainly by fluid currents, rather than by cellular shrinkage of the cortical vitreous, especially in later stage holes.

The importance of vitreous traction as a mechanism in macular hole formation remains controversial because there is not yet direct proof for this proposed mechanism. Guyer and Green[13] suggested that the tangential traction may occur by 3 possible mechanisms: fluid movements, cellular remodeling of cortical vitreous, and contraction of a cellular membrane on the inner surface of the cortical vitreous. Because fibrocellular membrane fragments were found in only 10% of the surgical specimens obtained from impending macular holes,[14] they hypothesized that fluid currents seemed to be a primary mechanism.[13] A histopathologic report with numerous surgically obtained specimens indirectly supports this hypothesis because fibrocellular and cellular membrane fragments were found in only a minority of the examined specimens.[15] A wavy line-shaped posterior vitreous face with folds that is attached to the peripheral

retina and inserts into the retina with a greater angle may suggest loosening rather than tightening of the posterior vitreous cortex and is consistent with such a hypothesis. However, because OCT is a static imaging method rather than a dynamic study like echography, the motion of the posterior vitreous face cannot be seen. It is possible to speculate that the wavy configuration of the posterior cortical vitreous is composed of relatively fixed folds and that there is a stiff vitreous face perhaps secondary to focal cellular proliferation and contracture analogous to proliferative vitreoretinopathy. At the time of this writing, the authors are examining cases at different points in time to determine if the wavy configuration is fixed or mobile (data not shown). Further longitudinal studies tracking vitreous face movements over brief periods are indicated.

A granular hyperreflective zone was evident in 50% to 60% of eyes with stage 1 or 2 holes. These were located in the peripheral vitreous where vitreoretinal separation was progressing. The incidence decreased to 33% in eyes with stage 3 or 4 holes. The granular hyperreflection may indicate structural changes of the cortical vitreous, including cellular remodeling and cellular proliferation in the cortical vitreous, as has been suggested by Guyer and Green.[13] The lower incidence of the granular hyperreflection in stage 3 to 4 holes and peripheral localization may be a consequence of the smaller chance of demonstrating fibrocellular and cellular membrane fragments in surgically excised specimens[13–15] compared with those in vitreomacular traction syndrome.[16–19] Although the role of a smooth curvature to the vitreous face remains unclear in the pathogenesis of macular hole development, structural changes in the peripheral vitreous may or may not induce contracture and tractional forces.

Another remarkable finding is the double-layered retinoschisis in the peripheral retina adherent to posterior vitreous cortex. The peripheral retina was split in the inner and outer plexiform nuclear layers. Interestingly, all zones of peripheral retinoschisis were evident only in the superior, supranasal, or supertemporal quadrants, or a combination thereof, in this small sample. Rhegmatogenous retinal detachment attributable to peripheral breaks with a concomitant noncausal macular hole occurs in approximately 1% to 3% of cases of retinal detachment.[20–22] Although the follow-up results have not been evaluated, the peripheral retinoschisis observed in 50% of stage 1 macular holes may be a potential explanation for a higher incidence of rhegmatogenous retinal detachments in the presence of noncausal macular holes. In addition, using the OCT montaging technique, a series of normal eyes at the different stages of posterior vitreous detachment was observed recently. During the process of posterior vitreous separation in normal eyes, there was no obvious peripheral retinoschisis observed (data not shown). These facts and the current study results suggest that the pathologic vitreoretinal adhesion in the eye with a macular hole is not limited in the macular region but also is in the peripheral retina.

In conclusion, montaged images of SD OCT in patients with macular hole demonstrated 2 different patterns of posterior vitreous configuration, as well as granular hyperreflection in the peripheral vitreous and areas of peripheral retinoschisis. The wavy posterior vitreous folds may provide further insight into the pathophysiology, development, and progression of idiopathic macular holes. These findings may provide a hypothesis implicating fluid currents, rather than by cellular remodeling, shrinkage of cellular membrane of the cortical posterior vitreous, or both as the source of anterior-to-posterior traction. Finally, the novel approach of montaging SD OCT images to examine relationships between the vitreous, retina, and associated structures adjacent to and outside of the macula may have a number of relevant applications in the study of vitreoretinal interface, paramacular, and macular pathologic features.

Acknowledgments. The authors thank Fumi Yamato, MD, and Tatsuya Deguchi, OP, for their help in recruiting the subjects and creating montage images of optical coherence tomography scans and Hiroto Kuroda, PhD, for his thoughtful comments regarding the fundamentals of optical coherence tomography.

References

1. Gass JD. Idiopathic senile macular hole: its early stages and pathogenesis. Arch Ophthalmol 1988;106:629–39.
2. Gass JD. Reappraisal of biomicroscopic classification of stages of development of a macular hole. Am J Ophthalmol 1995;119:752–9.
3. Smiddy WE, Michels RG, Glaser BM, de Bustos S. Vitrectomy for impending idiopathic macular holes. Am J Ophthalmol 1988;105:371–6.
4. Kelly NE, Wendel RT. Vitreous surgery for idiopathic macular holes: results of a pilot study. Arch Ophthalmol 1991; 109:654–9.
5. Wendel RT, Patel AC, Kelly NE, et al. Vitreous surgery for macular holes. Ophthalmology 1993;100:1671–6.
6. Puliafito CA, Hee MR, Schulman JS, Fujimoto JG. Optical Coherence Tomography in Ocular Diseases. Thorofare, NJ: SLACK Inc; 1996:17–34.
7. Hee MR, Puliafito CA, Wong C, et al. Optical coherence tomography of macular holes. Ophthalmology 1995;102: 748–56.
8. Mori K, Abe T, Yoneya S. Vitreoretinal tomography and foveolar traction in macular hole development and macular pseudohole [in Japanese]. Nihon Ganka Gakkai Zasshi 1999; 103:371–8.
9. Mori K, Abe T, Yoneya S. Dome-shaped detachment of premacular vitreous cortex in macular hole development. Ophthalmic Surg Lasers 2000;31:203–9.
10. Gaudric A, Haouchine B, Massin P, et al. Macular hole formation: new data provided by optical coherence tomography. Arch Ophthalmol 1999;117:744–51.
11. Chan A, Duker JS, Schuman JS, Fujimoto JG. Stage 0 macular holes: observations by optical coherence tomography. Ophthalmology 2004;111:2027–32.
12. Takahashi A, Yoshida A, Nagaoka T, et al. Macular hole formation in fellow eyes with a perifoveal posterior vitreous detachment of patients with a unilateral macular hole. Am J Ophthalmol 2011;151:981–9.
13. Guyer DR, Green WR. Idiopathic macular holes and precursor lesions. In: Franklin RM, ed. Retina and Vitreous: Proceedings of the Symposium on Retina and Vitreous, New Orleans, LA, USA, March 12–15, 1992. Amsterdam: Kugler; 1993:135–62.

14. Smiddy WE, Michels RG, De Bustos S, et al. Histopathology of tissue removed during vitrectomy for impending macular holes. Am J Ophthalmol 1989;108:360–4.
15. Sadda SR, Campochiaro PA, de Juan E Jr, et al. Histopathological features of vitreous removed at macular hole surgery. Arch Ophthalmol 1999;117:478–84.
16. Chang LK, Fine HF, Spaide RF, et al. Ultrastructural correlation of spectral-domain optical coherence tomographic findings in vitreomacular traction syndrome. Am J Ophthalmol 2008;146:121–7.
17. Gandorfer A, Rohleder M, Kampik A. Epiretinal pathology of vitreomacular traction syndrome. Br J Ophthalmol 2002; 86:902–9.
18. Shinoda K, Hirakata A, Hida T, et al. Ultrastructural and immunohistochemical findings in five patients with vitreomacular traction syndrome. Retina 2000;20:289–93.
19. Smiddy WE, Green WR, Michels RG, de la Cruz Z. Ultrastructural studies of vitreomacular traction syndrome. Am J Ophthalmol 1989;107:177–85.
20. Howard GM, Campbell CJ. Surgical repair of retinal detachments caused by macular holes. Arch Ophthalmol 1969;81:317–21.
21. Brown GC. Macular hole following rhegmatogenous retinal detachment repair. Arch Ophthalmol 1988;106:765–6.
22. Michels RG, Wilkenson CP, Rice TA. Retinal Detachment. St. Louis, MO: Mosby; 1990:629.

Footnotes and Financial Disclosures

Originally received: December 15, 2011.
Final revision: May 17, 2012.
Accepted: June 15, 2012.
Available online: August 11, 2012. Manuscript no. 2011-1793.

[1] Department of Ophthalmology, Saitama Medical University, Iruma, Saitama, Japan.

[2] Wilmer Eye Institute, Johns Hopkins University School of Medicine, Baltimore, Maryland.

Financial Disclosure(s):
The author(s) have no proprietary or commercial interest in any materials discussed in this article.

This research was supported in part by a grant-in-aid for scientific research from the Ministry of Education, Culture and Science in Japan (grant no.: 24592641; K.M.).

Correspondence:
Keisuke Mori, MD, PhD, Department of Ophthalmology, Saitama Medical University, 38 Morohongo, Moroyama, Iruma, Saitama, 350-0495, Japan. E-mail: keisuke@saitama-med.ac.jp.

Clinical Ophthalmology

Dovepress
open access to scientific and medical research

Open Access Full Text Article

ORIGINAL RESEARCH

Five-year results of photodynamic therapy with verteporfin for Japanese patients with neovascular age-related macular degeneration

Takashi Tsuchihashi
Keisuke Mori
Kazuhiro Ueyama
Shin Yoneya

Department of Ophthalmology, Saitama Medical University, Iruma, Saitama, Japan

Purpose: To describe the treatment outcome of photodynamic therapy (PDT) in Japanese patients with age-related macular degeneration (AMD) followed for 5 years.

Patients and methods: We retrospectively reviewed clinical charts of 51 patients with AMD. Thirty-one eyes of typical AMD (tAMD) and 20 eyes of polypoidal choroidal vasculopathy (PCV) were evaluated.

Results: The mean logarithm of the minimum angle of resolution (logMAR) vision of all AMD patients was 0.807 at the baseline examination and 0.937 at the 5 year examination. Mean visual acuity letter score loss is similar between patients with tAMD (−7.25) and with PCV (−5.36) at the month 60 examination. The patients with lesions of classic choroidal neovascularization (CNV) had 10.0 letters loss, but the patients with lesions of occult CNV had only 1.43 letters loss. The number of retreatments peaked in year 1 and declined immediately for patients with tAMD, but patients with PCV had significantly more frequent retreatments in the years 3 and 4 than patients with tAMD ($P = 1.48 \times 10^{-2}$, 5.96×10^{-3}, respectively).

Conclusion: Visual outcomes in patients with Japanese patients with AMD treated with PDT after 5-year follow up were worse than that in short-term follow up reported previously. In addition, the difference in visual prognosis between tAMD and PCV was not demonstrated after long-term follow-up.

Keywords: photodynamic therapy, age-related macular degeneration, polypoidal choroidal vasculopathy, visual outcomes

Introduction

Age-related macular degeneration (AMD) is the leading cause of severe visual loss in people over 50 years of age.[1] Photodynamic therapy (PDT) with verteporfin (Visudyne, Novartis Pharmaceutical Corporation, East Hanover, NJ, USA) is approved in more than 75 countries and commonly used to treat patients with subfoveal choroidal neovascularization (CNV) associated with AMD.[2–4] Several clinical trials in the United States and European countries have reported the benefits of PDT.[2,3,5–9] Guidelines for verteporfin therapy were based on the results of these trials in predominantly Caucasian populations. Although Treatment of Age-related Macular Degeneration with Photodynamic Therapy[5] (TAP) investigation reported a benefit at 24 months with respect to reducing the risk of three or more lines of visual acuity (VA) loss compared with placebo controls, the Japanese Age-Related Macular Degeneration Trial (JAT) study group[4] reported that PDT for CNV in. Sixty-four Japanese patients appeared to have better angiographic and visual outcomes than those of the Western trials.[2,3,5–9]

Polypoidal choroidal vasculopathy (PCV) is a distinct form of AMD, which meets the late age-related maculopathy (ARM) criteria of the International ARM

Correspondence: Keisuke Mori
Department of Ophthalmology, Saitama Medical University
38 Morohongo, Moroyama, Iruma, Saitama, 350-0495, Japan
Tel +81 492 76 1250
Fax +81 492 95 8002
Email keisuke@saitama-med.ac.jp

submit your manuscript | www.dovepress.com
Dovepress
http://dx.doi.org/10.2147/OPTH.S43566

Epidemiological Study Group,[10] but the phenotypic characteristics differ from typical neovascular AMD (tAMD). Over the past decade, the spectrum of neovascular AMD has been expanded to include PCV.[11–14] Patients with AMD in Japan have been reported to have PCV lesions more frequently than Caucasian patients[15–18] and PDT provides favorable results in the treatment of PCV.[19–23] Considering these outcomes of PDT treatments for PCV better outcomes are presumed for Japanese patients than Caucasian patients. Therefore, it is possible there may be a different response to PDT among different populations. Although TAP study provided the outcomes after PDT with AMD in the 5-year follow-up, JAT study[4] and JAT extension[24] have described up to 2 years follow-up information.

The purpose of this study is to provide the long-term follow-up information (5 years) after PDT in Japanese patients, and to compare the results with those of Western studies. We also explored whether the effect of PDT is different between patients with PCV lesion and those without.

Materials and methods

Subjects, examination and diagnosis

This retrospective study was conducted at Saitama Medical University, Saitama, Japan. All study subjects were unrelated Japanese Asian. All participants underwent a comprehensive ocular examination, including slitlamp biomicroscopy, funduscopy, contact lens biomicroscopic examinations of the retina, fluorescein and indocyanine green angiography, and optical coherence tomography (OCT) observation (Cirrus and Stratus, Carl Zeiss Meditec AG, Jena, Germany) at baseline and every 3-month visit. Every patient had fluorescein angiography at baseline. Regarding indocyanine green angiography, there were five exceptions, with a history of allergy for iodide, a positive result on pre-injection test or a known systemic problem such as liver disease, ischemic heart disease, cardiac arrhythmia or cardiac pacemakers. The differential diagnosis of tAMD and PCV was conducted so that if the polypoidal structure of the choroidal vessels with or without abnormal vascular networks was observed on indocyanine green angiography at the corresponding lesion on fluorescein angiography, the eyes were diagnosed as having PCV. We referred to the five cases without indocyanine green angiography, funduscopic appearance of typical orange-like polypoidal structure and OCT findings to make an accurate diagnosis.

Fifty-one consecutive patients who underwent initially PDT with the diagnosis of AMD between July 2004 and June 2005, with the completion of the month 60 examination, were recruited for this study. Inclusion criteria were as follows; (1) age of 50 years or older, (2) diagnosis of AMD in one or both eyes, (3) no association with other retinochoroidal diseases such as angioid streaks, high myopia (greater than 6D of myopic refractive error), central serous chorioretinopathy, presumed ocular histoplasmosis or retinal angiomatous proliferation (type 3 choroidal neovascularization). Excluded were the patients who had the treatments before and during the 5-year follow-ups with other methodologies; antivascular endothelial growth factor therapies, thermal laser photocoagulation, transpupillary thermotherapy, and/or vitreous surgery.

The main outcome of this study was best corrected visual acuity (BCVA) alteration during 5-year follow-up. We also analyzed the number of PDT retreatments. Recurrence of AMD was determined by a significant increase (20% or more compared with the lowest measurement at any previous scheduled visit) of the retinal thickness due to retinal edema and retinal detachment delineated by OCT measurement, increased or persistent fluorescein leakage from CNV or appearance of new retinal hemorrhage of one disc diameter or greater after 3 months or more. Additional retreatments were given if the CNV recurrence was observed as often as every 3 months during the 5-year follow-up.

Treatment procedures

The treatment protocol followed that used in the JAT study.[4] Treatment involved a 10 minute intravenous infusion of verteporfin, 6 mg/m^2 body surface area, followed by light exposure 15 minutes after the start of the infusion. Light exposure was given with a diode laser beam (639 ± 3 nm), delivered at 600 mW/cm^2 for 83 seconds to produce 50 J/cm^2.

Statistical analysis

The BCVA was determined using the Landolt C chart, and was calculated and presented as the logarithm of the minimum angle of resolution (logMAR) for statistical analyses and for conversion to letter scores. The following calculations were used:

- logMAR value = log10 (1/VA using Landolt C chart).
- Each 0.10 unit of logMAR difference = 5 letters.

The measured mean value of each group was compared using paired or unpaired *t*-test, chi-square test, and Bonferroni multiple comparison correction. $P < 0.05$ was considered to be statistically significant. All analysis was performed with commercially available software (SSRI version. 1.20, SSRI, Tokyo, Japan).